Univerzita Karlova

1. lékařská fakulta

Autoreferát disertační práce

UNIVERZITA KARLOVA
1. lékařská fakulta

Buněčný cyklus a diferenciace krvetvorných kmenových a progenitorových buněk

The cell cycle and differentiation of haematopoietic stem and progenitor cells

Mgr. Petr Páral

Praha 2019

Doktorské studijní programy v biomedicíně

Univerzita Karlova a Akademie věd České republiky

Obor: Fyziologie a patofyziologie člověka

Předseda oborové rady: Prof. MUDr. Jaroslav Pokorný, DrSc.

Školicí pracoviště: Ústav patologické fyziologie, 1. Lékařská fakulta, Univerzita Karlova

Školitel: RNDr. Luděk Šefc, CSc.

Konzultant: Prof. MUDr. Emanuel Nečas, DrSc.

Disertační práce bude nejméně pět pracovních dnů před konáním obhajoby zveřejněna k nahlížení veřejnosti v tištěné podobě na Oddělení pro vědeckou činnost a zahraniční styky Děkanátu 1. lékařské fakulty.

List of abbreviations

BFU-E	burst-forming unit-erythroid
BMCs	bone marrow cells
BrdU	5-bromo-2´-deoxy-uridine
BSA	bovine serum albumin
CFU-E	colony-forming unit-erythroid
c-Kit	CD117, stem cell factor receptor
CLPs	common lymphoid progenitors
CMPs	common myeloid progenitors
EdU	5-ethenyl-2´-deoxyuridine
FACS	fluorescence-activated cell sorting
GMPs	granulocyte-macrophage progenitors
HPCs	heterogeneous restricted progenitors
HSCs	haematopoietic stem cells
HSPCs	haematopoietic stem and progenitor cells
IMDM	Iscove's Modified Dulbecco's Medium
Lin	lineage
LSK	$Lin^{-}c\text{-}Kit^{+}Sca\text{-}1^{+}$
LS^{-}K	$Lin^{-}c\text{-}Kit^{+}Sca\text{-}1^{-}$
MEPs	megakaryocyte-erythroid progenitors
MPPs	multipotent progenitors
PBS	phosphate buffered saline
Sca-1	stem cell antigen
SLAM	signalling lymphocytic activation molecule, surface molecules CD150 and CD48

Content

List of abbreviations 3
Abstract 5
Abstrakt 6
1 Introduction 7
2 Hypothesis 10
Aims 10
3 Materials and methods 11
3.1 Experimental animals 11
3.2 Immunophenotyping of cell populations 11
3.3 Percentage of DNA-synthesizing cells determined by *in vitro* staining 11
3.4 Cell cycle analysis after *in vivo* staining of DNA synthesizing cells 11
3.5 Flow cytometry and cell sorting 12
3.6 Imaging flow cytometry 12
3.7 *In vitro* cultivation of erythroid progenitors in semi-solid media 12
4 Results 13
4.1 Determination of DNA synthesizing cell fraction in HSPC subpopulations 13
4.2 Cell cycle kinetics in HSPC subpopulations 14
4.3 Cell cycle and differentiation of erythroid progenitor and precursor cells 18
5 Discussion 24
5.1 Cell cycle and cell cycle kinetics of HSPCs 24
5.2 Erythroid developmental pathway in mouse bone marrow analysed by flow cytometry 25
6 Conclusions 27
7 References 28
8 List of Publications 31

Abstract

Haematopoietic stem and progenitor cells (HSPCs) are crucial for lifelong blood cell production. We analysed the cell cycle and cell production rate in HSPCs in murine haematopoiesis. The labelling of DNA-synthesizing cells by two thymidine analogues, optimized for *in-vivo* use, enabled the determination of the cell cycle flow rate into the G2-phase, the duration of the S-phase and the average cell cycle time in Sca-1$^+$ and Sca-1$^-$ HSPCs. The determination of cells with 2n DNA content and labelled during the preceding S-phase was used to establish the cell flow rates in the G1-phase. Our measurements revealed a significant difference in how Sca-1$^+$ and Sca-1$^-$ HSPCs self-renew and differentiate. The division of Sca-1$^+$ progenitors led to the loss of the Sca-1 marker in about half of newly produced cells, corresponding to asymmetric cell division. In contrast both Sca-1$^-$ progenitors, arising from mitotic cell division, entered a new round of the cell cycle. This corresponds to symmetric self-renewing cell division. The novel data also enabled us to estimate the cell production rates in the Sca-1$^+$ and in three subtypes of Sca-1$^-$ HSPCs.

We focused on adult murine erythroid differentiation in the next part of our study. We introduced an original flow cytometry approach for identifying and studying erythroid progenitor and precursor cells. This approach is based on the changing expression of two cell surface markers, c-Kit (receptor for stem cell factor) and CD71 (transferrin receptor 1) in bone marrow cells deprived of granulocytes, monocytes, lymphocytes and Sca-1$^+$ cells. We identified the early erythroid progenitor cells with BFU-E and CFU-E potentials within the cell population highly expressing c-Kit. The potential to give rise to BFU-E and CFU-E colonies was lost in the cells highly expressing CD71. Subsequently, erythroid differentiation progressed into the proerythroblasts which expressed c-Kit at a high level. Analysis of the cell cycle revealed that the differentiation of proerythroblasts into basophilic erythroblasts occurs in the course of a single cell cycle, in fact predominantly in the S-phase. During this S-phase, cells maintain the high expression of CD71 but rapidly lose the c-Kit marker and express the erythroid marker Ter119. The dual EdU-BrdU sequential labelling of DNA synthesizing cells, together with the metaphase block induced by colchicine, provide us with unique insights into the dynamics of cell proliferation and differentiation events in early erythroid cells.

Abstrakt

Krvetvorné kmenové a progenitorové buňky jsou nezbytné pro celoživotní produkci krevních buněk. Analyzovali jsme buněčný cyklus a intenzitu produkce těchto buněk v myší krvetvorné tkáni. Značení buněk syntetizujících DNA dvěma tymidinovými analogy, optimalizované pro *in vivo* použití, umožnilo stanovit rychlost, s jakou buňky vstupují do G2-fáze buněčného cyklu, výpočet délky trvání S-fáze a průměrné délky buněčného cyklu v Sca-1$^+$ a Sca-1$^-$ subtypech krvetvorných kmenových a progenitorových buněk. Diploidní buňky, které byly označeny v průběhu S-fáze předchozího buněčného cyklu, byly využity pro stanovení rychlosti, se kterou tyto buňky vstupují do G1-fáze buněčného cyklu. Tyto naše analýzy ukázaly významný rozdíl v sebeobnovném a diferenciačním charakteru buněčného dělení Sca-1$^+$ a Sca-1$^-$ buněk. Po rozdělení Sca-1$^+$ buněk asi polovina nově vzniklých buněk ztratila Sca-1, což odpovídá asymetrickému dělení. Oproti tomu, Sca-1$^-$ buňky se dělily sebeobnovným symetrickým dělením. Tyto nové údaje nám dále umožnily odhadnout rychlosti buněčných produkcí v Sca-1$^+$ buňkách a v 3 subtypech Sca-1$^-$ buněk.

V druhé části studie jsme se zaměřili na erytroidní diferenciaci kmenových a progenitorových buněk. Zavedli jsme nový způsob identifikace erytroidních progenitorů a prekurzorů v kostní dřeni a sledování průběhu jejich diferenciace. Tyto analýzy jsou založeny na měnící se expresi dvou povrchových znaků, c-Kit (receptor pro stem cell factor) a CD71 (transferinový receptor 1) na buňkách kostní dřeně, které byly zbaveny granulocytů, monocytů, lymfocytů a Sca-1$^+$ buněk. V buňkách vyznačujících se vysokou expresí c-Kit jsme prokázali časné erytroidní progenitory schopné tvořit kolonie BFU-E a CFU-E. Tato schopnost byla silně snížena v c-Kit$^+$ buňkách s nejvyšší expresí CD71. Na buňky obsahující BFU-E a CFU-E erytroidní progenitory navazuje stadium proerytroblastu, které stále intenzivně exprimuje c-Kit při současné vysoké expresi CD71. Analýzou buněčného cyklu bylo zjištěno, že následná diferenciace proerytroblastů do bazofilních erytroblastů se odehrává v průběhu jediného buněčného cyklu a to převážně v jeho S-fázi. V průběhu této S-fáze buňky udržují vysokou expresi CD71, rychle ztrácejí c-Kit receptor a zvyšují expresi erytroidního znaku Ter119. Metodika dvojitého značení buněk syntetizujících DNA pomocí EdU a BrdU, společně se zastavením buněk v stadiu metafáze kolchicinem, umožnily jedinečný náhled do dynamiky proliferace a diferenciace časných progenitorů a prekurzorů červených krvinek.

1 Introduction

Haematopoiesis is a highly efficient cell-producing system with a hierarchical structure consisting of haematopoietic stem cells (HSCs) at the apex, progenitors in the middle and differentiated precursors of blood cells at the bottom.

In the adult mouse, the population highly enriched by HSCs and haematopoietic progenitors can be identified through the expression of surface antigens discernible by monoclonal antibodies. These immature haematopoietic cells lack expression of the markers characteristic for lineages of differentiated myeloid and lymphoid blood cells (Lineage markers: CD3, Gr-1, Mac-1, B220, Ter119) and conversely express Sca-1 (Stem cell antigen) and c-Kit tyrosine kinase receptor for the cytokine stem cell factor (CD117). These are often abbreviated Lin^- $Sca\text{-}1^+c\text{-}Kit^+$ or LSK cell (Spangrude, Heimfeld and Weissman, 1988; Okada *et al.*, 1991; Ikuta and Weissman, 1992). The SLAM markers are the most frequently used to distinguish HSPCs with various specific developmental potentials. LSK cells are divided according to their CD150 and CD48 expression patterns to $CD150^+CD48^-$ haematopoietic stem cells (HSCs), $CD150^-CD48^-$ multipotent progenitors (MPPs), and two types of developmentally more restricted progenitors (HPCs-1 and HPCs-2) $CD150^-CD48^+$ and $CD150^+CD48^+$, respectively (Forsberg *et al.*, 2005; Kiel *et al.*, 2005; Weksberg *et al.*, 2008; Oguro, Ding and Morrison, 2013).

Whereas the LSK population contains the majority of primitive HSPCs, the loss of the Sca-1 antigen shifts this population to a more advanced progenitor pool. LS^-K cells lacking the IL7 receptor represent the developmentally advanced myeloid committed progenitors that are restricted in their developmental potential to granulocytes, macrophages, megakaryocytes and erythroid cells. LS^-K cells can be further divided according to the expression of CD34 and CD16_32 (FcγR III/II) to CMPs (common myeloid progenitors) $CD34^+CD16\_32^-$, GMPs (granulocyte-macrophage progenitors) $CD34^+CD16\_32^+$ and MEPs (megakaryocyte-erythroid progenitors) $CD34^-CD16\_32^-$ (Figure 1A) (Akashi *et al.*, 2000; Na Nakorn *et al.*, 2002). The lymphoid-biased progenitor population downstream of LSK are common lymphoid progenitors (CLP) $LS^{int.}K^{int.}IL7R^+$ (Kondo, Weissman and Akashi, 1997).

The sustained production of blood cells is the principal function of haematopoietic tissue. In mice, approximately 300 million bone marrow cells generate 200-250 million of various types of myeloid blood cells every day (Novak and Necas, 1994; Necas *et al.*, 1995). Traditionally, this enormous blood cell production had been thought to depend on the activity of HSCs,

which divide infrequently but maintain their population size by self-renewing cell divisions. The capacity for self-renewing cell divisions, either asymmetric or symmetric, had been regarded as a specific feature of HSCs that is lost with their differentiation.

A significant part of haematopoiesis represents the formation of red blood cells. Once the erythroid differentiation program is induced, MPPs give rise to CMPs and subsequently to MEPs, followed by two progenitors stages, traditionally identified via *in vitro* cultivation in semisolid medium, burst-forming units-erythroid (BFU-E) and colony-forming unit-erythroid (CFU-E) (Stephenson *et al.*, 1971; McLeod, Shreeve and Axelrad, 1974; Gregory and Eaves, 1978). The terminal erythroid differentiation occurs when proerythroblasts, the descendant of CFU-E cells, mature through the stages of basophilic, polychromatic to the orthochromatic erythroblasts that undergo enucleation, a process of nucleus removing, thus giving rise to the reticulocytes. Reticulocytes further autophagically remove organelles and extensively remodel their membrane to finally transform into erythrocytes (Dzierzak and Philipsen, 2013; Moras, Lefevre and Ostuni, 2017).

Thorough studies on the changes in the expression of surface antigens occurring during the early and terminal phases of erythropoiesis have allowed the immunophenotypic identification of individual erythroid progenitors by flow cytometry.

From this point of view, the most often used markers are Ter119 and transferrin receptor 1 (CD71). The Ter119 antigen is associated with glycophorin A and is detectable from the proerythroblastic stage to mature erythrocytes (Kina *et al.*, 2000). CD71 expression is initiated during the progenitor CFU-E stage, further enhanced upon the induction of hemoglobinization (i.e. in stages of proerythroblasts and erythroblasts), decreases in the reticulocyte stage and is lost in mature erythrocytes (Lok and Ponka, 2000; Pop *et al.*, 2010). Therefore, the expression pattern of CD71/Ter119 corresponds well to the maturation stages of proerythroblasts and erythroblasts during the terminal phase of erythropoiesis (Koulnis *et al.*, 2011).

Erythropoiesis is a process in which immature erythropoietic progenitors and precursors intensively proliferate and simultaneously differentiate to generate a sufficient number of fully matured red blood cells. However, the interrelation between cell cycle and differentiation remains poorly understood.

In this study, we conducted a thorough cell cycle analysis of HSPCs and erythroid progenitor and precursor cells in the adult bone marrow of mice. The sophisticated *in vivo* application of the dual-pulse sequential labelling of DNA using two thymidine analogues enabled us to reveal a link between the cell cycle and differentiation in HSPCs and also in erythroid progenitor and precursor cells.

2 Hypothesis

The sustained production of blood cells is the principal function of haematopoietic tissue. Blood cell production results from the intensive proliferation of haematopoietic cells. In mice, approximately 300 million bone marrow cells generate 200-250 million of various types of myeloid blood cells every day. The sustained production of blood cells is traditionally viewed as being derived from a miniscule supply of haematopoietic stem cells (HSCs). These stem cells possess self-renewal capacity or can differentiate into progenitor cells that further proliferate and differentiate into mature blood cells.

We hypothesize that self-renewing capacity is not confined to stem cells in the developmental hierarchy of haematopoietic stem and progenitor cells (HSPCs). We expect that an in-depth analysis of the cell cycle characteristics of HSPCs would provide novel information regarding the self-renewing capability of HSPCs.

The formation of red blood cells represents a significant part of haematopoiesis. In foetal liver haematopoiesis, the development of early erythroid cells has been reported to occur in the S-phase of the cell cycle.

We hypothesize that cell proliferation and differentiation are also closely linked during erythroid development in adult bone marrow. We expect that a thorough analysis of the cell cycle in early erythroid progenitors would uncover the relationship between the cell cycle and differentiation.

Aims

1. **To determine the proliferating rate in immunophenotypically defined populations of HSPCs and to compare it to their corresponding developmental hierarchy.**
2. **To introduce and optimize the dual thymidine analogue sequential DNA-labelling technique *in vivo* for the analysis of the proliferation and differentiation of HSPCs.**
3. **To semi-quantify the cell production arising from different haematopoietic subpopulations by determining the cell cycle parameters in various HSPCs.**
4. **To determine the interrelationship between the proliferation and differentiation of early erythropoietic progenitor cells by using the dual thymidine analogue sequential DNA-labelling technique.**

3 Materials and methods

3.1 Experimental animals

Male and female C57BL/6J mice 6-12 weeks of age were used.

3.2 Immunophenotyping of cell populations

Bone marrow was flushed from femurs of mice sacrificed by cervical dislocation with ice-cold solution of 1% bovine serum albumin in phosphate-buffered saline (PBS/BSA). Bone marrow cells (BMCs) (4 x 10^6 cells) were pelleted by centrifugation (400 g, 5 min, 4 °C) and cells in the pellet were incubated with a corresponding combination of fluorochrome-conjugated antibodies on ice for 30 min in the dark. Cells were then washed by PBS/BSA and resuspended in 250 µl of PBS/BSA.

3.3 Percentage of DNA-synthesizing cells determined by *in vitro* staining

An APC BrdU Flow kit was used to determine the percentage of various types of HSPCs and myeloid progenitors engaged in DNA synthesis, i.e. in the S-phase of the cell cycle. Four million of bone marrow cells were incubated for 45 min *in vitro* in 2 ml IMDM medium containing 10 µM BrdU (5-bromo-2´-deoxyuridine) (37°C, 5% CO_2 atmosphere). The bone marrow cells were then processed according to the APC BrdU Flow kit instructions.

3.4 Cell cycle analysis after *in vivo* staining of DNA synthesizing cells

To determine the cell flow rate into the G2-phase of the cell cycle, dual thymidine analogues sequential DNA-labelling with EdU and BrdU was applied. EdU (1.5 mg/mouse) and BrdU (2 mg/mouse) were administered intravenously (i.v.) separated by a time interval (T). Bone marrow was collected into an ice-cold PBS/BSA precisely 30 minutes after BrdU administration. The APC BrdU Flow Kit was used to process DNA-labelled cells. BrdU was detected by anti-BrdU antibody (MoBU-1 clone), EdU detection was performed with a Click-iT^{TM} Plus EdU Alexa Fluor 488 Flow Cytometry Assay Kit chemistry. The G2 cell flow rate was indicated by the percentage of EdU^+BrdU^- cells.

To determine the cell flow rate into the G1-phase of the cell cycle, mice were i.v. injected with 1 mg/mouse of BrdU, and after various time intervals (0.5-4.5 hours) bone marrow was

collected into ice-cold PBS/BSA. The APC BrdU Flow Kit was used to process DNA-labelled cells. The G1 cell flow rate was indicated by the percentage of 2n $BrdU^+$ cells.

Colchicine (0.05 mg/mouse) was administered intraperitoneally to arrest erythroid progenitor and precursor cells in metaphase. The dual thymidine analogues sequential DNA-labelling with EdU and BrdU as described in previous paragraph was applied 0.5 hours after colchicine administration.

3.5 Flow cytometry and cell sorting

Stained bone marrow cells were analyzed using a digital FACS Canto II flow cytometer, and a FACSAria IIu cell sorter. BD FACSDiva software version 6.1.3 or version 8.0.1 was used for data acquisition.

3.6 Imaging flow cytometry

Stained bone marrow cells were analyzed using 12 channels system AMNIS ImageStream X Mark II cytometer. INSPIRE system software was used for data collection. IDEAS analysis software was used for the analysis of collected data.

3.7 *In vitro* cultivation of erythroid progenitors in semi-solid media

MethoCult™ SF M3436 for murine erythroid BFU-E and and MethoCult™ M3334 for murine CFU-E progenitors were used. BMCs were sorted and platted on 30-mm Petri dishes in 1 ml of a semi-solid medium in concentrations 1 x 10^3 cells/ml (SF M3436) and 2 x 10^3 cells/ml (M3334). Two dishes were used for each progenitor sample and were kept 2 days (CFU-E) or for 12 days (BFU-E) at 37°C in a humidified atmosphere with 5% CO_2. Colonies were analysed and counted by phase contrast light microscopy and evaluated according to STEMCELL Technologies Mouse Colony-Forming Unit (CFU) Assays Technical Manual (v 3.2.0; Document # 28405).

4 Results

4.1 Determination of DNA synthesizing cell fraction in HSPC subpopulations

Flow cytometry was used to study early developmental stages of haematopoietic cells. The bone marrow cells were divided according to the expression of the Sca-1 marker into Sca-1$^+$ (LSK) and Sca-1$^-$ (LS$^-$K) subpopulations. LSK cells were further divided into four subpopulations according to their CD150 and CD48 expression patterns: haematopoietic stem cells (HSCs) CD150$^+$CD48$^-$, multipotent progenitors (MPPs) CD150$^-$CD48$^-$, and heterogeneous restricted progenitors (HPCs-1 and HPCs-2) CD150$^-$CD48$^+$ and CD150$^+$CD48$^+$, respectively (Kiel *et al.*, 2005; Oguro, Ding and Morrison, 2013). LS$^-$K cells lacking IL7R were characterized by CD34 and CD16_32 (FcγR III/II) markers as CMPs (common myeloid progenitors), GMPs (granulocyte-macrophage progenitors) and MEPs (megakaryocyte-erythroid progenitors) (Akashi *et al.*, 2000) (for gating see Figure 1A).

We determined pulse BrdU incorporation into immature bone marrow cells lacking lineage markers (Lin$^-$) and highly positive for c-Kit (Lin$^-$c-Kit$^+$ cells). The BrdU positive cells indicating the S-phase fraction of DNA-synthesizing cells ranged from 2.5±0.6% in MPPs to 64.8±2.3% in MEPs (Figure 1B, C).

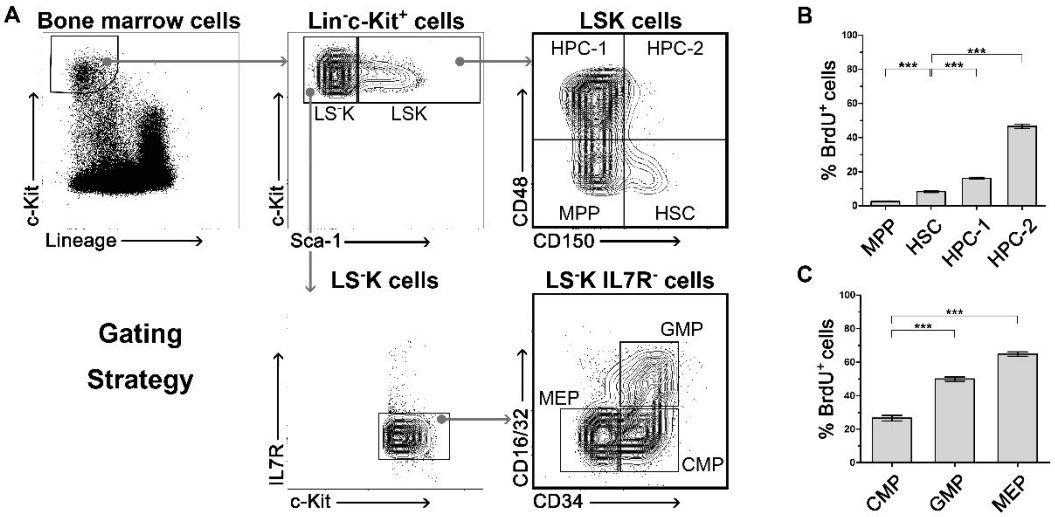

Figure 1 - Proliferation rate of various subtypes of LSK and LS$^-$K cells

A) *Gating strategy of Lin$^-$c-Kit$^+$ cells and of their subtypes in the Sca-1+ and Sca-1− fractions: HSC, MPP, HPC-1, HPC-2 and CMP, GMP, MEP.*

B) *BrdU$^+$ (S-phase) fraction after forty-five-minute in-vitro exposure to BrdU in LSK cells. Significant differences to HSCs (CD150+CD48− cells) are marked *** ($p < 0.001$) (n=8)*

C) *BrdU$^+$ (S-phase) fraction after forty-five-minute in-vitro exposure to BrdU in LS$^-$K cells. Significant differences to CMPss (CD150+CD48− cells) are marked *** ($p < 0.001$) (n=4)*

4.2 Cell cycle kinetics in HSPC subpopulations

We used the dual EdU-BrdU labelling technique to determine the duration of S-phase (T_S), cell flow rate into the G2-phase, and an average duration of the cell cycle (T_C) to further characterize the cell cycle features of HSPCs and to estimate their production rate. To achieve the labelling of all DNA synthesizing cells with EdU, i.e. those synthesizing DNA at the time of EdU administration and those which initiated DNA synthesis during the T_I interval (1.5 hours) preceding BrdU administration, we injected mice with a second dose of EdU 0.5 hours before injecting BrdU (see Figure 2A). The DNA labelling method, using two doses of EdU given 1 hour apart and T_I set at 1.5 hours, is graphically shown in Figure 2B.

The EdU^+BrdU^- cell fraction represents the cells leaving the S-phase (and thus entering into the G2-phase) during T_I and the EdU^+BrdU^+ cell fraction corresponds to the S-phase cell fraction. The G_2 flow rate, the S-phase cell duration and the average cell cycle duration were determined according the equation in the Figure 2C in all LSK cells and all LS^-K cells, in the LS^-K cells also in their three subtypes: CMPs, GMPs and MEPs (Figure 2D).

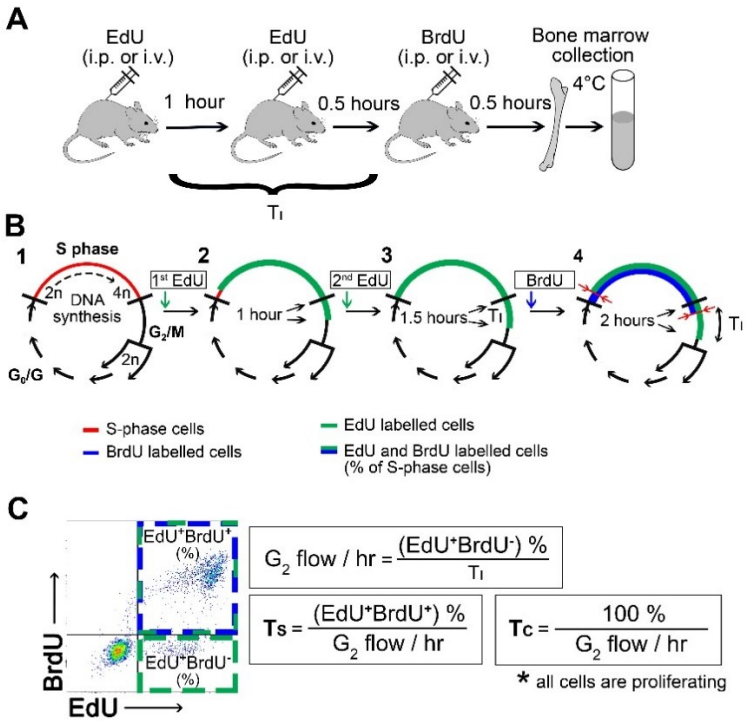

D

	LSK	LS^-K	CMP	GMP	MEP
G_2 flow / hour	2.2 ± 0.2	4.3 ± 0.5	2.4 ± 0.4	4.0 ± 0.4	6.0 ± 0.5
S-phase (hours)	7.8 ± 0.7	8.7 ± 0.6	8.7 ± 1.2	6.3 ± 0.5	9.8 ± 0.7
cell cycle (hours)	47.8 ± 4.9	23.4 ± 2.3	42.5 ± 7.3	24.9 ± 2.2	16.7 ± 1.3

Figure 2 - EdU-BrdU dual labelling of LSK and LS$^-$K cells and its use for cell cycle analysis of HSPCs

A) *Dual-deoxynucleoside labelling with two doses of EdU (2 x 1.5 mg/mouse) and single dose of BrdU (2 mg/mouse). Bone marrow cells were harvested 0.5 hours after BrdU administration.*

B) *EdU – BrdU dual labelling of DNA for in vivo cell cycle analysis of HSPCs (2 x EdU, T_I = 1.5 hours). 1: Cell cycle with highlighted S-phase (red), 2: EdU labels DNA (green) 0.5 hours after its administration and there are EdU unlabelled cells at the beginning of S-phase one hour after EdU (red), 3: 2nd EdU dose, given 0.5 hour before BrdU, ensures that all DNA-synthesizing cells are labelled with EdU (green) during T_I, 4: Half an hour after BrdU, all S-phase cells are double labelled by both EdU (green) and BrdU (blue). EdU-only labelled cells indicate the cells that exited from the S-phase during T_I.*

C) *Representative example of Lin$^-$c-Kit$^+$ cells plotted on EdU vs. BrdU diagram with color-highlighted gates (EdU$^+$BrdU$^-$ in the green gate, EdU$^+$BrdU$^+$ in the green/blue gate) corresponding to the EdU-BrdU labelling scheme depicted in B. The EdU$^+$BrdU$^-$ cells indicate the fraction of S-phase cells exiting the S-phase and thus entering into the G_2-phase within 1.5 hours (T_I) i.e. the G_2 cell flow rate. The total number of S-phase cells is indicated by EdU$^+$BrdU$^+$ cells. The S-phase duration (T_S) and the average cell cycle duration (T_C) are then calculated according the above equations.*

D) *G_2 cell flow rate, duration of S-phase (T_S) and the average cell cycle duration were determined in six mice (female). The results in the table are mean ± SEM.*

Further, we estimated the number of Lin$^-$c-Kit$^+$ cells generated by the mitotic division of cells previously labelled in the S-phase of the same cell cycle. Figure 3A shows how the flow rate of this cells can be determined. We labelled DNA-synthesizing cells in mice with a single dose of BrdU injected 0.5 - 4.5 hours prior to bone marrow collection and examined BrdU$^+$ cells with the diploid (2n) DNA content. DNA-synthesizing cells incorporate BrdU only for a short time after BrdU *in vivo* administration (approx. 0.5 hours). When the cells which have incorporated BrdU during the final part of the S-phase pass the G2-phase and mitotically divide, a new wave of 2n BrdU$^+$ cells appears and progressively increases as the cells which have incorporated BrdU in the middle and the early parts of S-phase divide and give rise to BrdU$^+$ cells with a 2n DNA content (Figure 3B).

BrdU$^+$ diploid cells appeared 1.5-2 hours after BrdU administration (Figure 3B) and their number increased linearly until 4.5 hours (Figure 3C). The slope of the linear regression reflecting the increase in the 2n BrdU$^+$ cell number, after its nadir corresponding to the duration of G2-phase and mitosis, reflects cells produced by mitotic division from those which have had incorporated BrdU at the time of its administration.

We determined the flow rates of 2n BrdU$^+$ cells for all HSPC subpopulations according to the curve slopes of the linear regressions reflecting the increase in the 2n BrdU$^+$ cell number. Our expectation that the increment in 2n BrdU$^+$ cells per hour, i.e. the cell flow rate into the (G0)G1-phase, should be twice as high as the cell flow rate into the G2-phase in particular cell

types, due to the doubling effect of mitosis was not confirmed. Our experimental data differed from this theoretical value of 2.0 both in LSK cells, where it was only 1.1, and also in LS$^-$K cells, where it was 2.4-2.9 (Figure 3D).

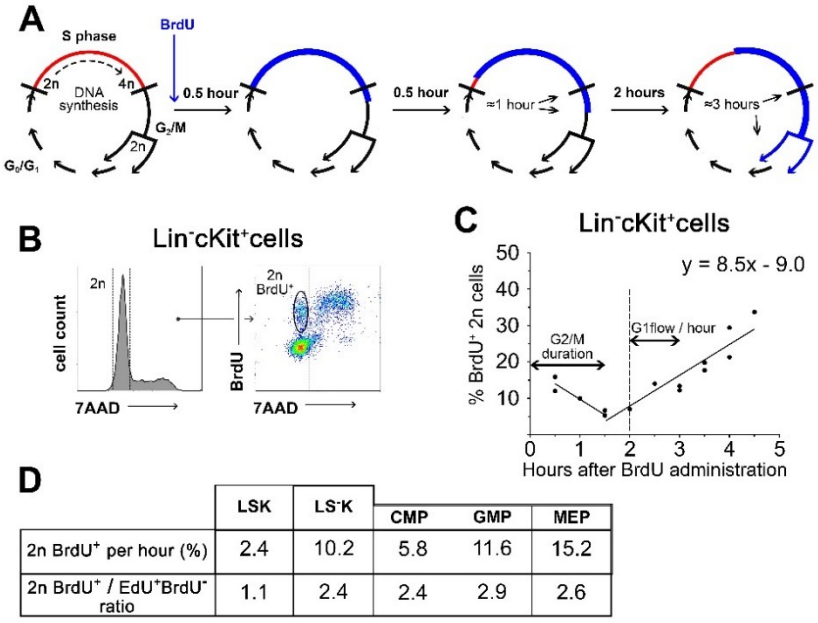

D

	LSK	LS$^-$K	CMP	GMP	MEP
2n BrdU$^+$ per hour (%)	2.4	10.2	5.8	11.6	15.2
2n BrdU$^+$ / EdU$^+$BrdU$^-$ ratio	1.1	2.4	2.4	2.9	2.6

Figure 3 – Flow rate of 2n BrdU$^+$ cells entering into the (G0)G1-phase determined in HSPCs

A) *Schematic image showing the principle of measuring of the cell outflow from mitosis (red: cells with unlabelled DNA, blue: cells with BrdU-labelled DNA).*

B) *Representative 7AAD histogram and BrdU / 7AAD dotplot of Lin$^-$cKit$^+$ cells depicting gating strategy for 2n daughter cells.*

C) *Results of the analysis of Lin$^-$c-Kit$^+$ bone marrow cells. Changes in 2n BrdU$^+$ cells frequency depending on time elapsed since BrdU administration. Results from three independent experiments were pooled. The points were fitted to a line by linear regression, and the equation of increasing line is listed in graph (n=15).*

D) *2n BrdU$^+$ increment per hour, i.e. G1 flow rate, determined according to curve slopes and ratio of G1 flow rate vs G2 flow rate for each HSPC type.*

Previous results showed that almost half of LSK cells lost the Sca-1 antigen after mitotic division because the cell flow rate into G1-phase was only 1.1 times that in the preceding G2 phase, instead of the expected value of 2.0. This corresponds to asymmetric cell division where one cell replaces the cell that had divided and the other cell differentiates into another (LS$^-$K) cell type. In contrast, in LS$^-$K cells and in their CMPs, GMPs and MEPs subtypes, the cell flow rate into the G1-phase was more than 2.0 times that in the preceding G2 phase, which indicated that a majority of the LS$^-$K cells arising from mitotic division entered a new round of the cell cycle while both preserving their phenotype, i.e. the mitosis was symmetric and self-

renewing. Furthermore, there is indication for an additional external influx of LS$^-$K cells, presumably from a part of LSK cells that lost Sca-1 marker after/during mitosis (Figure 4A).

The calculation of cell production rates used the total number of a particular cell type in bone marrow (N) determined from the number of the cells in the femoral bone marrow multiplied by 15 (bone marrow in 1 femur represents ≈ 6.7% of the total bone marrow (Novak and Necas, 1994).

Other experimentally determined values used for estimation of the cell production rate in subtypes of Lin$^-$c-Kit$^+$ immature haematopoietic cells were their cell flow rates into the G2- (G2) and G1-phases (G1) of the cell cycle and the G1/G2 ratio (R). The cells produced per hour in the entire bone marrow are then calculated as N x G2 x R/100 (Figure 4B).

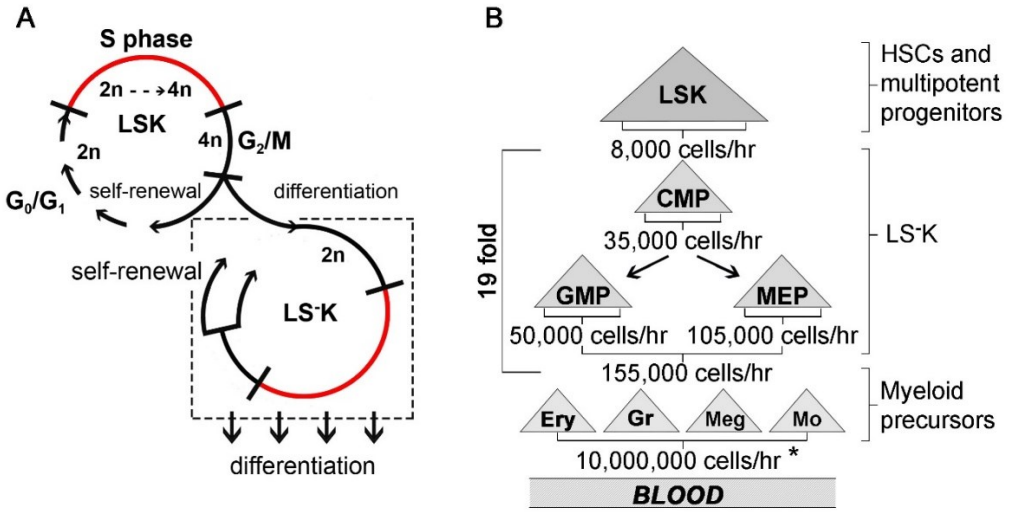

Figure 4 – A model of self-renewal and differentiation in LSK and LS$^-$K cells and estimation of cell production in hierarchy of HSPCs and myeloid precursors of blood cells

A) *Cell division in LSK cells is primarily asymmetric when one cell becomes an LS$^-$K cell, while the other enters a new self-renewing cell cycle. LS$^-$K cells undergo self-renewal leading to their amplification and receive an influx of cells from the asymmetrically dividing LSK cells. The differentiation of LS$^-$K cells is not linked to cell division.*
B) *Developmental hierarchy within HSPCs with established cell production rates and the average multiplication factor in the compartment of LS$^-$K cells and in the maturing precursors of red blood cells, granulocyte/monocytes and megakaryocytes. The cells produced per hour are calculated as described in Results.*

4.3 Cell cycle and differentiation of erythroid progenitor and precursor cells

We have established a new approach for identifying individual erythroid-progenitor stages within the bone marrow cells.

We discriminated erythroid progenitors in the bone marrow cells lacking the expression of the lineage markers (B220, Gr-1, Mac-1), the marker of immature HSPCs (Sca-1) and the granulocyte-macrophage-progenitor marker (CD16_32). These $B220^{-}$/$Gr\text{-}1^{-}$/$Mac\text{-}1^{-}$/$Sca\text{-}1^{-}$/$CD16\_32^{-}$ bone marrow cells were then divided into 10 erythroid-progenitor gates according to their c-Kit and CD71 expression (Figure 5A).

The cells in gates 0 – 5 were investigated for their capacity to form erythroid colonies. Cells in gate 0, immunophenotypically corresponding to CMPs and MEPs, exhibited the highest BFU-E potential that was decreased in gate 1 and lost in gate 2. The highest CFU-E potential was possessed by cells in gate 1 and also lost in gate 2 (Figure 5B).

To further characterise the progenitors and nucleated precursors of red blood cells, we used the imaging flow cytometry technology and cell criteria established by McGrath et al. (2008). This approach is an alternative to the traditional microscopic classification of erythroid progenitors and enables erythroid progenitors to be distinguished according to the changes in their cell size, density of the surface-expressed antigen Ter119, in their nuclear size, and in the intensity of Draq5 stained DNA reflecting the degree of nuclear condensation. Figure 5C projects erythroid progenitor and precursor cells in gates 0 - 9 into the fields established by McGrath et al. (2008) for various developmental stages of nucleated precursors of red blood cells. Cells from gates 0 – 2, highly expressing c-Kit together with the initiation of CD71 expression, increase their cell and nuclear size and gradually differentiate into proerythroblasts (ProE). Cells from gates 3 – 4 lose c-Kit and initiate a strong Ter119 expression. They progress into the stage of basophilic erythroblasts. Cells in gates 5 – 9 progressively reduce their CD71 expression, shrink the cell and nuclear sizes, pass through the stage of polychromatic erythroblasts to the last nuclear erythroid precursor: orthochromatic erythroblasts.

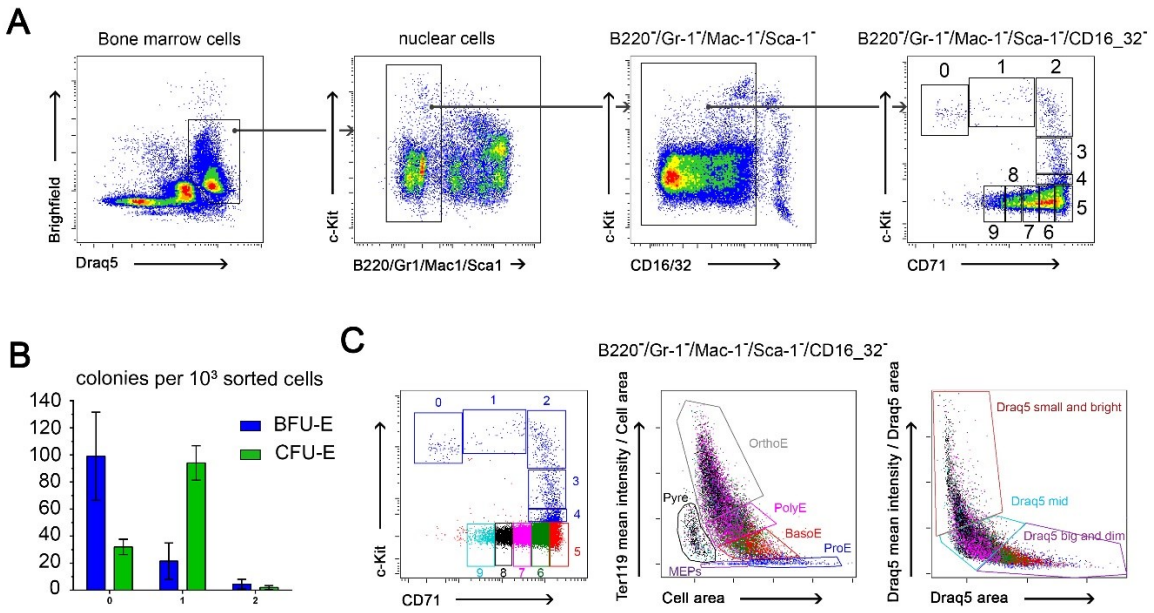

Figure 5 – Identification of erythroid progenitor and precursor cells in bone marrow

A) *Representative flow-cytometry analysis of erythroid progenitor and precursor cells in a murine bone marrow.*
B) *BFU-E and CFU-E colony-forming potential of cell in gates 0 – 5. 10^3 sorted cells from each of gates 0 - 5 were in vitro cultured in duplicates on a 30-mm Petri dish in a culture medium optimized for burst-forming unit-erythroid (BFU-E, SF M3436 medium). $2x10^3$ sorted cells from each of gates 0 - 5 were in vitro cultured in duplicates on a 30-mm Petri dish in a culture medium optimized for colony-forming unit-erythroid (CFU-E, M3334 medium). BFU-E colonies were scored on day 12, CFU-E colonies on day 2. Results are pooled from two independent experiments.*
C) *The B220⁻/Gr-1⁻/Mac-1⁻/Sca-1⁻/CD16_32⁻ bone marrow cells were analysed according to their changing cell size (middle dot-plot) and progressive nuclear condensation (right dot-plot). This gating strategy for distinguishing of nuclear erythroid progenitor and precursor cells was adopted from the study published by McGrath et al. (2008).*

To examine the cell cycle status of erythroid progenitors and precursors, we administered i.v. BrdU to mice and harvested bone marrow after 30 min. The bone marrow was processed to show the BrdU cell labelling against their DNA content, which doubled during the S-phase of the cell cycle from 2n into 4n value.

Figure 6A shows the cell cycle status in erythroid progenitors and precursors divided according to their c-Kit and CD71 expression into ten gates. For a more detailed analysis of the cell cycle within each gate, we divided the S-phase cell fraction into 3 parts according to the increasing amount of synthesized DNA: early S-phase cells, middle S-phase cells and late S-phase cells. The S-phase cells were relatively uniformly distributed in its early, middle and late parts except for the cells in gates 2 – 4. While cells from gates 2 and 3 were in the early and middle S-phase, cells from gate 4 were mostly in the late S-phase (and G2/M-phase) (Figure 6A). These findings

strongly suggest that the transition of cells from gate 2 to gate 4 occurs during their passage through the S-phase of a single cell cycle.

Further, we determined the mean fluorescence intensity (MFI) of fluorochrome-conjugated antibodies against CD71, c-Kit and Ter119 antigens in the cells from gates 0 – 9. The S-phase fraction increased from 7.8 ± 1.8 % in cells from gate 0 to > 90 % in cells with the highest CD71 expression level (gates 2 – 5) and then declined together with diminishing CD71 expression in cells from gates 6 – 9. The expression of c-Kit is, after its initial up-regulation in cells in gates 1 and 2, strongly down-regulated in gate 3 when cells synthesize DNA in the early and middle part of the S-phase. There is a rapid onset of the Ter119 expression in cells which progressed into the late S-phase in gate 4 (Figure 6B, C).

These results suggest that increased CD71 expression and initiation of DNA synthesis in the early S-phase are required for the differentiation of cells from the MEP stage to proerythroblasts appearing in gate 2 (Figure 5C) and that the differentiation of proerythroblasts into the basophilic erythroblasts present in gate 4 is associated with a steep loss of c-Kit expression during the progression of cells through the S-phase. In contrast, Ter119 was rapidly up-regulated during this S-phase.

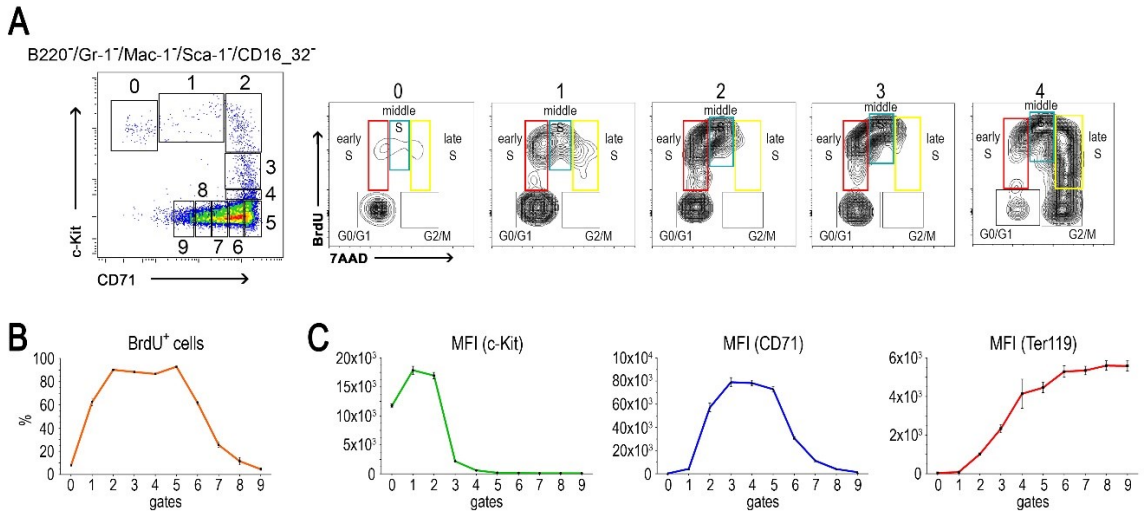

Figure 6 – Cell cycle analysis of erythroid progenitor and precursor cells

A) *B220⁻/Gr-1⁻/Mac-1⁻/Sca-1⁻/CD16_32⁻ bone marrow cells were divided according to their c-Kit and CD71 expression into ten gates (0 – 9) containing erythroid progenitor and precursor cells and their cell cycle status is depicted on representative 7AAD / BrdU dotplots.*

B) *BrdU⁺ (S-phase) cell fraction frequency and G0/G1 cell fraction frequency determined in erythroid progenitor and precursor cells in gates (0 – 9) (n=10)*

C) *Mean fluorescence intensity (MFI) of c-Kit, CD71 and Ter119 was analysed in erythroid progenitor and precursor cells in gates (0 – 9) (n=4).*

To clarify how $CD71^-$ megakaryocyte-erythroid progenitor (MEP) cells develop into $Ter119^+$ erythroid cells and how this is linked to the progression of the cells through the cell cycle, we double-labelled DNA-synthesizing cells with EdU followed by BrdU 3 hours later and analysed the distribution of the labelled cells in progressively differentiating erythroid cells in gates 1 - 4 (Figure 5A).

The time interval of 3 hours that separated the EdU and BrdU administration, was chosen to allow the passage of the cells labelled with EdU at the end of the S-phase through the G2- and M-phases and into postmitotic cells with their DNA content reduced from 4n to 2n and thus clearly distinguishable (EdU labelled diploid cells) (Figure 7A).

The BrdU vs. 7AAD diagram is a snapshot of cells taken 0.5 hours after BrdU injection which shows their actual distribution into the G0/G1- S- and G2/M-phases of the cell cycle. The EdU label marks cells which synthesized DNA 3 hours before the BrdU injection. Hence, by examining the EdU-labelled cells in the BrdU vs. 7AAD diagram, we introduce a time factor into the cell cycle analysis of the studied cells.

A proportion of the G0/G1-phase cells in gate 1 was EdU^+. These cells originated from the mitotic division of the cells that synthesized DNA before 3 hours (and were either from gate 0 or gate 1). The cells from gate 1 which were in the S-phase ($BrdU^+$) contained two EdU^+ cell fractions that were clearly distinguishable by their low or a high DNA content. The EdU^+ cells with the DNA content close to 2n (in the early S-phase) synthesized DNA 3 hours earlier in the previous cell cycle, mitotically divided and initiated a new round of DNA synthesis in the next cell cycle. The EdU^+ cells with the DNA content close to 4n (in the late S-phase) incorporated EdU 3 hours earlier and were still in the S-phase after 3 hours when BrdU was administered (Figure 7B).

We similarly analyzed cells in gates 2 – 4. This revealed that all G1-phase cells (2n) were EdU^+ in these cell populations. This demonstrates that the transition of cells from gate 1 into gate 2 and 3, characterized by a further significant increase in the expression of CD71, is accompanied by cell division. The S-phase cells in gates 2 and 3 consisted predominantly of the cells which incorporated EdU 3 hours earlier in the S-phase of the previous cell cycle. The cells in gate 4 are synchronized in the middle and late parts of the S-phase (see Figure 7B). They contain a few EdU^+ cells which incorporated EdU 3 hours earlier. These cells still synthesized DNA when BrdU was administered, which means that the S-phase lasts >3 hours. The analysis of cells from gates 2 - 4 thus demonstrates that (1) the transition of cells from

gate 1 to gates 2/3 requires cell division and (2) that the S-phase to next S-phase transition only takes ≈ 2 hours (or even less, because a significant portion of S-phase cells from the previous cells cycle and the next cell cycle overlap, although the time interval between EdU and BrdU administration was only 3 hours), (3) the significant transition in the cell immunuphenotype occurring in gates 2 - 4 takes place in the course of a single S-phase (Figure 7D).

To further extend this our dynamic cell cycle analysis, we blocked the mitotic division with colchicine, an inhibitor of microtubule polymerization, which arrests cells in metaphase during their mitotic division (TAYLOR, 1965). Colchicine (0.05 mg/mouse) was given 0.5 hours before the EdU injection which was then followed, after 3 hours, by BrdU injection (Figure 7A). The administration of colchicine resulted in a disruption of erythroid differentiation in c-Kit$^+$ and CD71 highly positive cells, thus in cells intensively proliferating (Figure 7C). Figure 7B shows the accumulation of 4n cells in the G2/M-phase, in gates 1 and 4. Importantly, the interruption of the influx of EdU$^+$ cells into the next S-phase in gates 2 and 3 strongly supports our finding that a cell division is required for the transition of cells from gate 1 into gates 2 and 3.

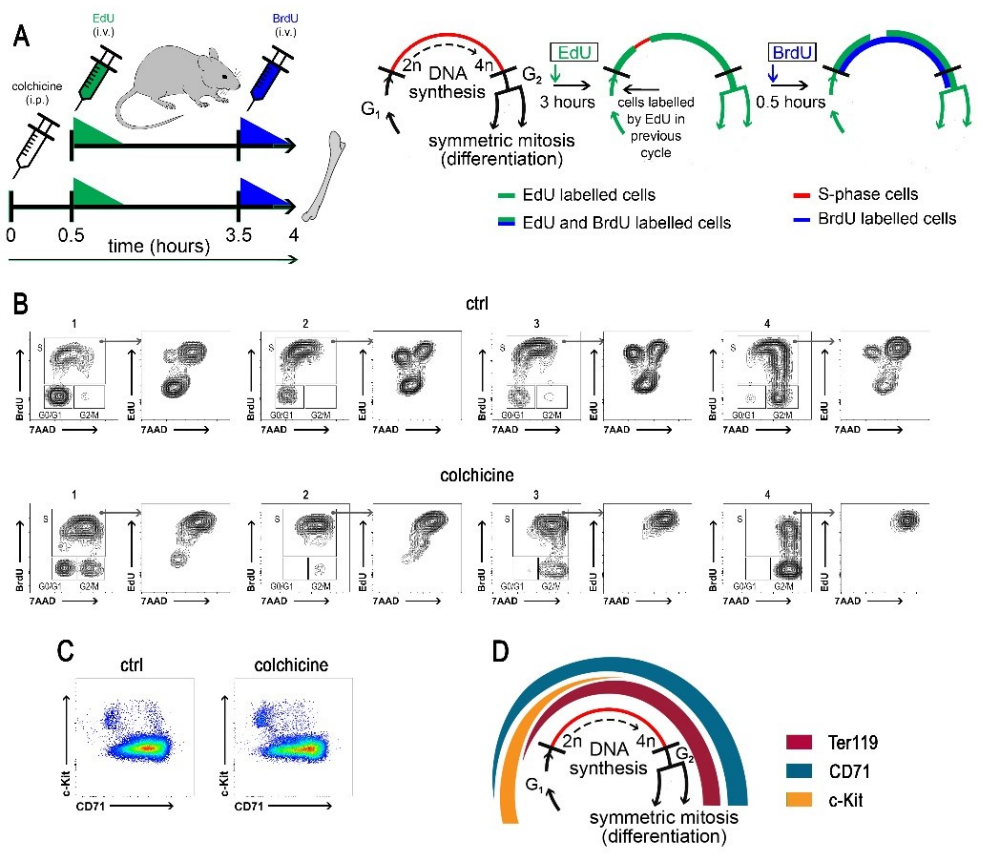

Figure 7 – Dynamic cell cycle analysis of erythroid progenitor and precursor cells in control and colchicine treated mice

A) 0.5 hours after *Colchicine administration (0.05 mg/mouse) dual-deoxynucleoside labelling was performed with a single EdU (1.5 mg/mouse) and single BrdU dose (2 mg/mouse) separated by 3 hours. Bone marrow cells were harvested 0.5 hours after the administration of BrdU. Green and blue triangles illustrate the short-term pulse character (approx. 0.5 hours) of EdU and BrdU labelling. A schematic image showing the principle of EdU and BrdU labelling used in this experimental setting is shown on the right.*
B) *Cells from gates 1 - 4 of B220$^-$/Gr-1$^-$/Mac-1$^-$/Sca-1$^-$/CD16_32$^-$ bone marrow cells of control and colchicine-treated mice were plotted on the BrdU vs 7AAD diagram and cell-cycle phases were discriminated. The EdU incorporation was further analysed in S-phase cells.*
C) *Representative examples of B220$^-$/Gr-1$^-$/Mac-1$^-$/Sca-1$^-$/CD16_32$^-$ bone marrow cells of control and colchicine-treated mice.*
D) *Erythroid differentiation steps after mitotic division of cells in population 1 occur during single cell cycle in cells from gates 2 – 4.*

5 Discussion

5.1 Cell cycle and cell cycle kinetics of HSPCs

Haematopoietic tissue is characterized by intensive cell proliferation, resulting in the lifelong production of mature blood cells. The longevity of blood cell production is due to the presence of HSCs possessing both self-renewal and differentiation multilineage developmental potential. However, HSCs in the bone marrow of adult mice divide very rarely (Wilson *et al.*, 2007; Foudi *et al.*, 2009; van der Wath *et al.*, 2009). Therefore, HSCs are linked to blood cell production through actively proliferating progenitor cells. We attempted to estimate the quantitative contribution of various types of these immature haematopoietic cells to steady-state murine haematopoiesis.

To achieve this goal, we optimized the sequential dual labelling of DNA-synthesizing cells with EdU and BrdU for *in vivo* use for determining the cell flow rates into the G2-phase in various types of HSPCs. These enabled us to determine the duration of the S-phase and to calculate the average cell cycle time in LSK cells and in three subtypes of LS^-K cells: CMPs, GMPs and MEPs.

We further decided to check to check the obtained values by independently determining the number of daughter cells arising from their mitotic division. Therefore, we measured the increment of cells with 2n DNA content labelled with BrdU during the preceding S-phase.

The obtained experimental results significantly differed from the expectation that both daughter cells arising from mitosis would maintain the phenotype of the mother cell. Furthermore, they differed in the opposite ways in LSK and LS^-K cells. While newly-produced 2n LSK cells were only 1.1 times their cell flow into the G2-phase, there were seemingly more than 2.0 times in newly-produced LS^-K cells. Neither of the values fitted the model of one cell giving rise to two identical daughter cells during its division. Almost half of the total progeny of LSK cells lost the LSK phenotype, which strongly suggested that they differentiated in mitosis. Moreover, there must have been an external source of influx of 2n LS^-K cells in addition to their generation by their own cell division. This led us to formulate a model in which LSK cells self-renew and differentiate into LS^-K cells by predominantly asymmetric cell divisions (Figure 4A).

Our research, designed primarily to establish the quantitative cell production in various types of haematopoietic progenitor cells, has achieved this goal, as summarized in Figure 4B.

Unexpectedly, it revealed the significant difference in how the Sca-1$^+$ and Sca-1$^-$ subsets of immature haematopoietic cells self-renew and differentiate. While the LSK cells maintain their population size and differentiate to LS$^-$K cells by asymmetric cell divisions, the LS$^-$K cells primarily amplify their numbers by symmetric self-renewing cell divisions.

5.2 Erythroid developmental pathway in mouse bone marrow analysed by flow cytometry

We devised a new approach for the identification and analysis of the erythroid developmental pathway in the bone marrow of adult mice. Instead of the CD71/Ter119 cells profiling that is effective in the foetal liver, we utilised the c-Kit/CD71 profiling in the bone marrow (Figure 5A).

We used the imaging flow cytometry to characterize the cells plotted in the c-Kit/CD71 diagram with respect to their morphology corresponding to various developmental stages of erythroid precursor cells as developed by McGrath et al. (2008) (Figure 5C).

The analysis of the cell cycle in immature Sca-1 positive HSPCs and in their Sca-1 negative progeny suggested that while Sca-1 positive cells lose the Sca-1 antigen during mitosis, Sca-1 negative cells differentiate in the course of the cell cycle (part 4.2, (Páral *et al.*, 2018)). Therefore, we decided to analyse how Sca-1 negative myeloid progenitors initiate differentiation into erythroid progenitors and red blood cell precursor cells.

Our results indicate that the early erythroid differentiation is connected with the induction of intensive cell proliferation and with DNA synthesis in the S-phase of the cell cycle (Figure 6A, B). These findings are consistent with erythroid differentiation in the foetal liver, where the up-regulation of CD71 coincides with the synchronization of the last generation of CFU-E cells in the S-phase that is necessary for their further differentiation into proerythroblasts (Pop *et al.*, 2010).

Our results also demonstrate that the differentiation of proerythroblasts (cells in gate 2) into basophilic erythroblasts (cells in gate 4) occurs during the S-phase within a single cell cycle.

To analyse the early phases of erythroid differentiation taking place in c-Kit positive cells in more detail and to introduce a dynamic factor into our analysis, we applied the dual sequential labelling method of DNA synthesizing cells with EdU and BrdU (Figure 7A).

We analysed cells labelled with EdU according to their DNA content. This distinguished between cells which were in the early phase of the S-phase with DNA content close to 2n and

cells cells with DNA content close to 4n (in late S-phase), which had incorporated EdU when it was administered and were still in the S-phase of the same cell cycle three hours later. Cells in the gates 2 and 3 contained a significant fraction of EdU^-labelled cells that started a new round of DNA synthesis within three hours, while cells in the gate 4 predominantly contained EdU-labelled cells that were in the early S-phase during EdU administration and after three hours they still synthesized DNA in the final part of the same S-phase. These results confirm our previous conclusion that the cells that undergo the significant phenotypic development between gate 2 and gate 4 perform these changes in parallel with the replication of their genetic material (in the S-phase of a single cell cycle).

We used colchicine, a drug that arrests cells in the metaphase during mitosis and thus interrupts cell division and the initiation of the next cell cycle, to further enhance this dynamic approach to cell cycle analysis in erythroid progenitor cells.

The mitotic block lasting 3.5 hours induced by colchicine led to the accumulation of 4n cells in gate 1 and abolished the appearance of EdU^+ cells in gates 2 and 3. This treatment also interfered with the erythroid differentiation exemplified by the augmentation of the CD71 expression occurring between cells in gate 1 and gates 2 and 3 (Figure 7B, C). This further demonstrates that the early phase of erythroid differentiation is tightly linked with their progression through the cell cycle and, particularly, with the reduplication of the cell genetic material in the S-phase of the cell cycle.

6 Conclusions

The present study provides experimental evidence that

- the fraction of DNA-synthesizing cells is a characteristic feature of various types of HSPCs
- the double-pulse DNA labelling with EdU and BrdU requires optimization for *in vivo* use, then it represents a convenient tool for determining the cell cycle kinetic parameters
- the LSK cells maintain their population size and differentiate to $LS^{-}K$ cells by symmetric cell divisions
- the $LS^{-}K$ cells primarily amplify their numbers by symmetric self-renewing cell divisions
- the immunophenotypic identification based on c-Kit/CD71 profiling enables to investigate the development of erythroid progenitors into differentiated precursors of red blood cells
- the differentiation of proerythroblasts into basophilic erythroblasts occurs during S-phase within a single cell cycle

7 References

Akashi, K. *et al.* (2000) 'A clonogenic common myeloid progenitor that gives rise to all myeloid lineages.', *Nature*, 404(6774), pp. 193–7. doi: 10.1038/35004599.

Dzierzak, E. and Philipsen, S. (2013) 'Erythropoiesis: Development and Differentiation', *Cold Spring Harbor Perspectives in Medicine*, 3(4), pp. a011601–a011601. doi: 10.1101/cshperspect.a011601.

Forsberg, E. C. *et al.* (2005) 'Differential Expression of Novel Potential Regulators in Hematopoietic Stem Cells', *PLoS Genetics*, 1(3), p. e28. doi: 10.1371/journal.pgen.0010028.

Foudi, A. *et al.* (2009) 'Analysis of histone 2B-GFP retention reveals slowly cycling hematopoietic stem cells.', *Nature biotechnology*, 27(1), pp. 84–90. doi: 10.1038/nbt.1517.

Gregory, C. J. and Eaves, A. C. (1978) 'Three stages of erythropoietic progenitor cell differentiation distinguished by a number of physical and biologic properties.', *Blood*, 51(3), pp. 527–37.

Ikuta, K. and Weissman, I. L. (1992) 'Evidence that hematopoietic stem cells express mouse c-kit but do not depend on steel factor for their generation.', *Proceedings of the National Academy of Sciences of the United States of America*. National Academy of Sciences, 89(4), pp. 1502–6.

Kiel, M. J. *et al.* (2005) 'SLAM family receptors distinguish hematopoietic stem and progenitor cells and reveal endothelial niches for stem cells.', *Cell*, 121(7), pp. 1109–21. doi: 10.1016/j.cell.2005.05.026.

Kina, T. *et al.* (2000) 'The monoclonal antibody TER-119 recognizes a molecule associated with glycophorin A and specifically marks the late stages of murine erythroid lineage.', *British journal of haematology*, 109(2), pp. 280–7.

Kondo, M., Weissman, I. L. and Akashi, K. (1997) 'Identification of clonogenic common lymphoid progenitors in mouse bone marrow.', *Cell*, 91(5), pp. 661–72.

Koulnis, M. *et al.* (2011) 'Identification and Analysis of Mouse Erythroid Progenitors using the CD71/TER119 Flow-cytometric Assay', *Journal of Visualized Experiments*, (54). doi: 10.3791/2809.

Lok, C. N. and Ponka, P. (2000) 'Identification of an Erythroid Active Element in the Transferrin Receptor Gene', *Journal of Biological Chemistry*, 275(31), pp. 24185–24190. doi: 10.1074/jbc.M000944200.

McGrath, K. E., Bushnell, T. P. and Palis, J. (2008) 'Multispectral imaging of hematopoietic cells: Where flow meets morphology', *Journal of Immunological Methods*, 336(2), pp. 91–97. doi: 10.1016/j.jim.2008.04.012.

McLeod, D. L., Shreeve, M. M. and Axelrad, A. A. (1974) 'Improved plasma culture system for production of erythrocytic colonies in vitro: quantitative assay method for CFU-E.', *Blood*, 44(4), pp. 517–34.

Moras, M., Lefevre, S. D. and Ostuni, M. A. (2017) 'From Erythroblasts to Mature Red Blood Cells: Organelle Clearance in Mammals', *Frontiers in Physiology*, 8, p. 1076. doi: 10.3389/fphys.2017.01076.

Na Nakorn, T. *et al.* (2002) 'Myeloerythroid-restricted progenitors are sufficient to confer radioprotection and provide the majority of day 8 CFU-S.', *The Journal of clinical investigation*, 109(12), pp. 1579–85. doi: 10.1172/JCI15272.

Necas, E. *et al.* (1995) 'Hematopoietic reserve provided by spleen colony-forming units (CFU-S).', *Experimental hematology*, 23(12), pp. 1242–6.

Novak, J. P. and Necas, E. (1994) 'Proliferation-differentiation pathways of murine haemopoiesis: correlation of lineage fluxes', *Cell Proliferation*. Blackwell Publishing Ltd, 27(10), pp. 597–633. doi: 10.1111/j.1365-2184.1994.tb01377.x.

Oguro, H., Ding, L. and Morrison, S. J. (2013) 'SLAM family markers resolve functionally distinct subpopulations of hematopoietic stem cells and multipotent progenitors.', *Cell stem cell*, 13(1), pp. 102–16. doi: 10.1016/j.stem.2013.05.014.

Okada, S. *et al.* (1991) 'Enrichment and characterization of murine hematopoietic stem cells that express c-kit molecule.', *Blood*, 78(7), pp. 1706–12.

Páral, P. *et al.* (2018) 'Cell cycle and differentiation of Sca-1 $^{+}$ and Sca-1 $^{-}$ hematopoietic stem and progenitor cells', *Cell Cycle*. Taylor & Francis, 17(16), pp. 1979–1991. doi: 10.1080/15384101.2018.1502573.

Pop, R. *et al.* (2010) 'A Key Commitment Step in Erythropoiesis Is Synchronized with the Cell Cycle Clock through Mutual Inhibition between PU.1 and S-Phase Progression', *PLoS Biology*. Edited by M. A. Goodell, 8(9), p. e1000484. doi: 10.1371/journal.pbio.1000484.

Spangrude, G. J., Heimfeld, S. and Weissman, I. L. (1988) 'Purification and characterization of mouse hematopoietic stem cells.', *Science (New York, N.Y.)*, 241(4861), pp. 58–62.

Stephenson, J. R. *et al.* (1971) 'Induction of colonies of hemoglobin-synthesizing cells by erythropoietin in vitro.', *Proceedings of the National Academy of Sciences of the United States of America*. National Academy of Sciences, 68(7), pp. 1542–6.

TAYLOR, E. W. (1965) 'THE MECHANISM OF COLCHICINE INHIBITION OF MITOSIS. I. KINETICS OF INHIBITION AND THE BINDING OF H3-COLCHICINE.', *The Journal of cell biology*, 25, p. SUPPL:145-60.

van der Wath, R. C. *et al.* (2009) 'Estimating Dormant and Active Hematopoietic Stem Cell Kinetics through Extensive Modeling of Bromodeoxyuridine Label-Retaining Cell Dynamics', *PLoS ONE*. Edited by A. Leri, 4(9), p. e6972. doi: 10.1371/journal.pone.0006972.

Weksberg, D. C. *et al.* (2008) 'CD150- side population cells represent a functionally distinct population of long-term hematopoietic stem cells', *Blood*, 111(4), pp. 2444–2451. doi: 10.1182/blood-2007-09-115006.

Wilson, A. *et al.* (2007) 'Dormant and self-renewing hematopoietic stem cells and their niches.', *Annals of the New York Academy of Sciences*, 1106, pp. 64–75. doi: 10.1196/annals.1392.021.

8 List of Publications

Publications with relation to the thesis

1. Páral P, Faltusová K, Molík M, Renešová N, Šefc L, Nečas E. Cell cycle and differentiation of Sca-1 + and Sca-1 − hematopoietic stem and progenitor cells. Cell Cycle. 2018;17(16):1979–91. doi: 10.1080/15384101.2018.1502573. **IF = 3.304**

2. Páral P, Báječný M, Savvulidi F, Nečas E. Cell Cycle Analysis Using In Vivo Staining of DNA-Synthesizing Cells. Methods Mol Biol. 2019. doi: 10.1007/7651_2019_228. **IF = 1.465**

Other publications

1. Hofer M, Pospíšil M, Hoferová Z, Komůrková D, Páral P, Savvulidi F, Sefc L. The pharmacological activation of adenosine A1 and A3 receptors does not modulate the long- or short-term repopulating ability of hematopoietic stem and multipotent progenitor cells in mice. Purinergic Signal. 2013;9(2):207–14. doi: 10.1007/s11302-012-9340-5. **IF = 3.19**

2. Loukotová L, Kučka J, Rabyk M, Höcherl A, Venclíková K, Janoušková O, Páral P, Kolářová V, Heizer T, Šefc L, Štěpánek P, Hrubý M. Thermoresponsive β-glucan-based polymers for bimodal immunoradiotherapy – Are they able to promote the immune system? J Control Release. 2017;268:78–91. doi: 10.1016/j.jconrel.2017.10.010. **IF = 7.877**

3. Faltusová K, Szikszai K, Molík M, Linhartová J, Páral P, Šefc L, Savvulidi F, Nečas E. Stem Cell Defect in Ubiquitin-Green Fluorescent Protein Mice Facilitates Engraftment of Lymphoid-Primed Hematopoietic Stem Cells. Stem Cells. 2018;36(8):1237–48. doi: 10.1002/stem.2828. **IF = 5.587**